Seasonal and Interannual Temperature Variations in Nares Strait, North-West Greenland

A. Münchow[1]

Abstract. July 9, 2012.

1. Introduction

Greenland's ice-sheet is a prominent feature of the global climate system. Its topographic relief influences global-scale atmospheric circulation [*Woollings*, 2010], its freshwater discharge in the form of meltwater [*Hanna et al.*, 2008], icebergs [*Broecker*, 1994], and ice islands [*Johnson et al.*, 2011] potentially impact the global meridional overturning circulation in the ocean and sealevel rise. Upper bounds of global sealevel rise due to a shrinking ice-sheet were initially estimated to be 1-2 m by 2100 [*Pfeffer et al.*, 2008], but more systematic and comprehensive recent analyses by *Moon et al.* [2012] suggest a more modest impact of less than 0.1 m global sealevel rise by 2010 due to Greenland's retreating tidewater glaciers.

Both ocean and atmosphere also impact the ice-sheet around its margins via melting of tidewater glaciers from the ocean below [*Rignot and Steffen*, 2008; *Holland et al.*, 2008; *Hanna et al.*, 2009] and the atmosphere above [*Mote*, 2007; *Mernild et al.*, 2011]. Satellite observations document change of retreating glaciers [*Moon et al.*, 2012] that is most profound in the southern part of Greenland [*Joughin et al.*, 2010], but these changes are spread towards north-west of Greenland [*Khan et al.*, 2010], the focus of the this study.

Northern Greenland separates two pathways of atmospheric and oceanic exchange between the Arctic and North-Atlantic Oceans. To the east of Greenland lies Fram Strait, a 500 km wide and 3000 m deep opening between Greenland and Spitsbergen while to the west lies Nares Strait, a 40 km wide and 300 m deep opening between Greenland and the Canadian Archipelago. While these geographic scales suggest that most exchange of water and ice takes place via the deeper and wider Fram Strait, dynamical constraints involving ocean stratification and the earth's rotation imply that either pathway is wide and deep enough to accommodate similar exchange via semi-geostrophic boundary currents found both off eastern Greenland [*Sutherland and Pickart*, 2008; *Sutherland et al.*, 2009] and eastern Baffin Island [*LeBlond*, 1980; *Tang et al.*, 2004; *Smith*, 1931]. Both currents advect cold and fresh water as well as ice and icebergs southward along the east coast of Greenland and Baffin Island. The generally cyclonic ocean circulation on both sides of Greenland suggests large spatial correlation scales along topographic features such as shelves and continental slopes [*Chapman and Beardsley*, 1989; *Greene et al.*, 2008] .

Within this context we ask, if it is possible to detect and identify regional temperature changes of the atmosphere-ice-ocean system within Nares Strait over the last decade. Nares Strait facilitates the generally southward movement of air [*Samelson and Babour*, 2008], ice [*Kwok et al.*, 2010], and water [*Münchow and Melling*, 2008] from the Lincoln Sea of the Arctic Ocean to the north of Greenland into Baffin Bay which connects to the Arctic Ocean (Figure 1). A preliminary study of ocean temperatures at the bottom of Nares Strait near 350 m depth revealed statistically significant warming at that depth [*Münchow et al.*, 2011b] for the 2003-09 period. We here generalize that study by considering the entire water column along with remotely sensed ice or sea surface temperatures, as well as available coastal surface air temperature records. We analyze observational data from an incomplete network of surface air stations starting in 1950, thermal satellite remote sensing starting in 2000, and a limited ocean mooring array starting in 2003.

2. Data

The National Climatic Data Center distributes daily surface air station data. Table 1 lists details of all records from northern Greenland and Ellesmere Island longer than 10 years at elevations less than 100 meters whose location is shown in Figure 1. Records contain substantial gaps in time ranging from days to decades. The records from Thule Air Force Base and Eureka is most complete with almost continuous coverage since 1950, the Alert record starts at the same time, but has gaps, most prominent from 1960-1977. Stations at Grise Fjord, Carey Islands, Kap Morris Jesup, and Station Nord were not started until the 80s. In the absence of a better observational record, we will define mean temperatures as well as annual and semi-annual cycles as climatological normal against which we will compare observations from the 21st century as anomalies.

The Moderate Resolution Imaging Spectroradiometer (MODIS) flown aboard the Terra satellite provides almost continuous measurements of radiation in 36 optical and infra-red frequency bands starting in February of 2000 at spatial resolution of 1 km at its nadir. The polar orbiting, sun-synchronous satellite provides about 8-12 scenes each day of northern Greenland with a repeat orbit every 16 days. The National Aeronautical and Space Agency (NASA) distributes the raw Level-0 as well the altitude and ephemeris data in near real time in segments of 5 minutes along the flight path. For each day within the 16-day orbit cycle we select one daily 5 minute segment for processing. Using open-source, public domain software provided by NASA and the HDF Group, we convert these raw data to geo-located Level-1B data in engineering units.

A major challenge of optical and thermal MODIS data relates to clouds obstructing the view to the surface of the earth. Standard cloud products designed for mid-latitude applications are often of little use at polar latitudes in the presence of ice, snow, and temperature inversions during polar night. Verification and calibration data are often lacking for polar applications, especially during the months of polar night. Using prior work by *Ackerman et al.* [2010]; *Frey et al.* [2008]; *Liu et al.* [2004] we implement 5 cloud tests as well as 3 clear-sky tests that use MODIS bands at 3.9, 6.7, 7.2, 11, 12, and 13 μm at each pixel. For polar day over water and ice we implement an additional test for the reflective band at $0.865\mu m$, i.e., we required $R_{0.865} \leq 0.08$

[1]College of Marine Studies, University of Delaware, Newark, Delaware, USA.

0148-0227/12/$9.00

to pass our screening. Table 2 lists details of these tests as implemented.

We calculate MODIS surface temperatures following an Arctic algorithm that *Vincent et al.* [2008] developed for the marginal ice zone of our study area. Using ship-mounted radiometers to calibrate space-borne radiometers, *Vincent et al.* [2008] use brightness temperatures T_{11} from the infrared channel near $11.03\mu m$ to decide if the reflecting surface is ice ($T_{11} \leq -4.2°C$) or water ($T_{11} \geq -2.2°C$). Ice surface temperatures IST are calculated following *Key et al.* [1997] split-window technique using coefficient provided by *Riggs et al.* [2006] while sea surface temperatures SST_{Arctic} are calculated as

$$SST_{Arctic} = -4.012372 + 1.016284 \times T_{11} - 273.15 \quad (1)$$

where T_{11} is in Kelvin. Temperatures between the ice and sea surface temperatures are linearly interpolated between IST and SST_{Arctic} using T_{11} to complete the Composite Arctic Sea Surface Temperature Algorithm (CASSTA). *Vincent et al.* [2008] describe details and demonstrate its superior performance in the southern Nares Strait region.

The ocean data originate from instruments moored on the ocean floor to measure currents, temperature, salinity, and pressure within the water column at discrete locations on a single section across southern Kennedy Channel (Figure 1). Kennedy Channel is at the center of Nares Strait and is located north of the 225-m sill depth connecting Nares Strait to the Atlantic Ocean while it is to the south of the 290-m sill depth connecting Nares Strait to the Arctic Ocean [*Münchow et al.*, 2011a]. The instruments were deployed for 3 years 2003-06 and 2 years 2007-09. The velocity moorings consist of 75 kHz acoustic Doppler current profilers (ADCP) which estimate current vectors from the bottom to within about 30-m of the surface at 30 minutes intervals in 8-m vertical bins. The hydrographic moorings contain discrete SeaBird 37SM sensors from which to estimate temperature, salinity, and pressure at 15 minute intervals. More detailed descriptions of instrumentation and initial data processing can be found in *Münchow and Melling* [2008] and *Rabe et al.* [2010] for velocity and hydrographic moorings, respectively, and thus are not repeated here.

3. Surface Air Temperature

Figure 2 shows the annual cycle for a northern and southern meteorological stations on Greenland (Thule and Morris Jesup) and Ellesmere Island (Grise Fjord and Alert) along with the number of years that records are available for each 10-day segment of the year. We interpret each data year as an independent sample or degree of freedom from which to estimate upper and lower limits at 95% confidence which we show in Figure 2 for the mean for that day of the year.

The southern location of Thule and longer periods of open water elevates both summer and winter temperatures relative the stations. This moderating ocean warming is even more pronounced at the Carey Islands about 80 km to the west of Thule (not shown). The two stations along the Arctic Ocean, Alert and Morris Jesup as well as Station Nord (not shown) further to the east are almost identical in their climatological means except for the short summer period when air temperatures at Alert are about 1.5 °C warmer and similar to Grise Fjord about 550 km to the south. For a more systematic and quantitative analysis we select a common 1987-2010 observational period for which a concurrent record is most complete. *Lesins et al.* [2010] provides a detailed description of a single station, Eureka, for the 1953-2007 period.

Table 3 summarizes the statistics for each station. The 1987-2010 mean temperatures vary from $-8.8 \pm 1.0°C$ on the Carey Islands offshore of Thule to -16.9 ± 1.4 at Kap Morris Jesup at the northern tip of Greenland. We define a seasonal cycle as,

$$T_s(t) = T_1 cos(\omega_1 t - \phi_1) + T_2 cos(\omega_2 t - \phi_2) \quad (2)$$

where $T_s(t)$ is the seasonal temperature T_s as a function of time t. This oscillations with two frequencies ω_1 and $\omega_2 = 2\omega_1$ represent the annual cycle and its first harmonic, respectively. These cycles have amplitudes T_i and phases ϕ_i $(i = 1, 2)$ that we determine by minimizing the least-square error between the irregular spaced data and the fit. Table 3 indicates a dominantly annual oscillation that varies between 12 °C in the south and 17°C in the north on Greenland with almost constant phase. The semi-annual cycle is a first small correction of 1-4 °C representing seasonal asymmetries, that is, a shorter spring precedes the temperature maximum while a longer fall follows it. Figure 3 shows temperature time series for Alert. The most striking feature is the much enhanced variance during the winter when daily temperature fluctuations of over 10 °C are not uncommon.

No long term climate change signal is apparent to the eye, but a large and significant warming trend is contained in these records nevertheless. We extract this signal after we remove the seasonal temperature T_s analyzing $T_a = T - T_s$ as anomalies T_a where T is the raw daily data. T_a contains interannual signals, weather, as well as instrument noise. We find the linear trend T_{rend} as

$$T(t) = T_0 + T_{rend} \times t \quad (3)$$

as well as a constant offset T_0 that relates to the mean temperature. Substantial and statistically significant (95% level) temperature trends of about $0.1 \pm 0.05°C$ emerge from all available stations (Table 3). Figure 4 visualizes these trends of uniform warming of all stations. We thus conclude that the air around coastal Greenland and Ellesmere Island north of 76° latitude has warmed by about 0.11 ± 0.025 °C per year or by about 2.4 ± 0.57 °C since 1987. This uniform warming around northern Greenland and Ellesmere Island is not steady, however, but is peculiar to the 1987-present period. Where longer records are available, such as for Alert, Thule, and Eureka, we find for the 1951-2010 period barely significant trends that are only 20% of those observed for the 1987-2010 period. Nevertheless, these data reveal spatial uniformity of surface air properties at seasonal and interannual time scales. Furthermore, a similar warming trend for several decades was observed in the 1920s over much of the North Atlantic Ocean poleward of 60°N latitude. The changes then correlated with a weakening Icelandic Low that also moved southward [*Rogers*, 1985]. Such changes relate to the North Atlantic Oscillation(NAO) index [**?**], however, interannual fluctuations for the 1987-2010 period are largely uncorrelated with the NAO (Figure 4) and perhaps indicative of a more global warming signal.

4. Surface Ice and Ocean Temperature

Figure 7 shows our 10-year-long record of daily brightness temperature at a single pixel location of the generally ice-covered center of Nares Strait near 66.7 W longitude and 80.8 N latitude. Both seasonal and interannual variations are pronounced and will be discussed below.

5. Hydrography

6. Circulation

7. Discussion

7.1. Under-ice water mass structure

8. Conclusions

Acknowledgments. We acknowledge financial and in-kind support from the Canadian Federal Programme for the International Polar Year (IPY 2006-SR1-CC-135), Fisheries and Oceans Canada and the USA National Science Foundation. We are also extremely grateful for the enthusiastic and professional support of captain, crew, scientists and technicians on the USCGC Healy in 2003 (HLY031), and aboard the CCGS Henry Larsen in 2007 and 2009. HLJ is funded by a Royal Society University Research Fellowship. .

References

Ackerman, S., R. Frey, K. Strabala, Y. Liu, L. Gumley, B. Baum, and P. Menzel, Discriminating clear-sky from cloud with MODIS Algorithm Theoretical Basis Document (MOD35), *Tech. rep.*, Cooperative Institute for Met. Sat. Stud, Univ. Wisconsin- Madison, 2010.

Broecker, W. S., Massive iceberg discharges as triggers for global climate-change, *Nature*, *372*, 421–424, 1994.

Chapman, D. C., and R. C. Beardsley, On the origin of shelf water in the Middle Atlantic Bight, *J. Phys. Oceanogr.*, *19*, 384–391, 1989.

Frey, R. A., S. A. Ackerman, Y. H. Liu, K. I. Strabala, H. Zhang, J. R. Key, and X. G. Wang, Cloud detection with MODIS. Part I: Improvements in the MODIS cloud mask for collection 5, *Journal of Atmospheric and Oceanic Technology*, *25*, 1057–1072, 2008.

Greene, C., J. Pershing, T. Cronin, and N. Ceci, Arctic climate change and its impacts on the ecology of the North Atlantic, *Ecology*, *89 Suppl.*, S24–S38, 2008.

Hanna, E., P. Huybrechts, K. Steffen, J. Cappelen, R. Huff, C. Shuman, T. Irvine-Fynn, S. Wise, and M. Griffiths, Increased runoff from melt from the Greenland ice sheet: A response to global warming, *Journal of Climate*, *21*, 331–341, 2008.

Hanna, E., J. Cappelen, X. Fettweis, P. Huybrechts, A. Luckman, and M. H. Ribergaard, Hydrologic response of the Greenland ice sheet: the role of oceanographic warming, *Hydrological Processes*, *23*, 7–30, 2009.

Holland, D. M., R. H. Thomas, B. De Young, M. H. Ribergaard, and B. Lyberth, Acceleration of Jakobshavn Isbrae triggered by warm subsurface ocean waters, *Nature Geoscience*, *1*, 659–664, 2008.

Johnson, H., A. Münchow, K. Falkner, and H. Melling, Ocean circulation and properties in Petermann Fjord, Greenland, *J. Geophys. Res.*, *116*, C01,003, 2011.

Joughin, I., B. E. Smith, I. M. Howat, T. Scambos, and T. Moon, Greenland flow variability from ice-sheet-wide velocity mapping, *Journal of Glaciology*, *56*, 415–430, 2010.

Key, J. R., J. B. Collins, C. Fowler, and R. S. Stone, High-latitude surface temperature estimates from thermal satellite data, *Remote Sensing of Environment*, *61*, 302–309, 1997.

Khan, S. A., J. Wahr, M. Bevis, I. Velicogna, and E. Kendrick, Spread of ice mass loss into northwest Greenland observed by GRACE and GPS, *Geophysical Research Letters*, *37*, L06,501, 2010.

Kwok, R., L. T. Pedersen, P. Gudmandsen, and S. S. Pang, Large sea ice outflow into the Nares Strait in 2007, *Geophys. Res. Let.*, *37*, L03,502, 2010.

LeBlond, P. H., On the surface circulation in some channels of the Canadian Arctic Archipelago, *Arctic*, *33*, 189–197, 1980.

Lesins, G., T. J. Duck, and J. R. Drummond, Climate trends at Eureka in the Canadian High Arctic, *Atmosphere-Ocean*, *48*, 59–80, 2010.

Liu, Y. H., J. R. Key, R. A. Frey, S. A. Ackerman, and W. P. Menzel, Nighttime polar cloud detection with MODIS, *Remote Sensing of Environment*, *92*, 181–194, 2004.

Mernild, S. H., T. L. Mote, and G. E. Liston, Greenland ice sheet surface melt extent and trends: 1960-2010, *Journal of Glaciology*, *57*, 621–628, 2011.

Moon, T., I. Joughin, B. Smith, and I. Howat, 21st-century evolution of Greenland outlet glacier velocities, *Science*, *336*, 576–578, 2012.

Mote, T. L., Greenland surface melt trends 1973-2007: Evidence of a large increase in 2007, *Geophysical Research Letters*, *34*, L22,507, 2007.

Münchow, A., and H. Melling, Ocean current observations from Nares Strait to the west of Greenland: Interannual to tidal variability and forcing, *J. Mar. Res.*, *66 (6)*, 801–833, 2008.

Münchow, A., K. Falkner, and H. Melling, Baffin Island and West Greenland Current systems in northern Baffin Bay: Synoptic observations and climatological context, *J. Phys. Oceanogr.*, *submitted*, xxx, 2011a.

Münchow, A., K. K. Falkner, H. Melling, B. Rabe, and H. L. Johnson, Ocean warming of Nares Strait bottom waters off northwest Greenland, 2003-2009, *Oceanography*, *24*, 114–123, 2011b.

Pfeffer, W. T., J. T. Harper, and S. O'Neel, Kinematic constraints on glacier contributions to 21st-century sea-level rise, *Science*, *321*, 1340–1343, 2008.

Rabe, B., A. Münchow, H. Johnson, and H. Melling, Nares Strait hydrography and salinity field from a 3-year moored array, *J. Geophys. Res.*, *115*, 2010.

Riggs, G., D. Hall, and V. Salomonson, MODIS Sea Ice Products Guide to Collection 5, *Tech. rep.*, National Snow and Ice Data Center, 2006.

Rignot, E., and K. Steffen, Channelized bottom melting and stability of floating ice shelves, *Geophys. Res. Let.*, *35*, L02,503, 2008.

Rogers, J. C., Atmospheric circulation changes associated with the warming over the northern North Atlantic in the 1920s, *J. Climate Appl. Meteor.*, *24*, 1303–1310, 1985.

Samelson, R., and P. Babour, Low-level winds in Nares Strait: a model-based mesoscale climatology, *Mon. Weather Rev.*, *136*, 4746–4759, 2008.

Smith, E., *The Marion expedition to Davis Strait and Baffin Bay, Scientific results, part 3*, Bulletin No. 19, United States Government Printing Office, Washington, DC, 1931.

Sutherland, D. A., and R. S. Pickart, The East Greenland Coastal Current: Structure, variability, and forcing, *Progr. Oceanogr.*, *78*, 58–77, 2008.

Sutherland, D. A., R. S. Pickart, E. P. Jones, K. Azetsu-Scott, A. J. Eert, and J. Olafsson, Freshwater composition of the waters off southeast Greenland and their link to the Arctic Ocean, *J. Geophys. Res.*, *114*, C05,020, 2009.

Tang, C. C. L., C. K. Ross, T. Yao, B. Petrie, B. M. DeTracey, and E. Dunlap, The circulation, water masses and sea-ice of Baffin Bay, *Progr. Oceanogr.*, *63*, 183–228, 2004.

Vincent, R. F., R. F. Marsden, P. J. Minnett, K. A. M. Creber, and J. R. Buckley, Arctic waters and marginal ice zones: A composite Arctic sea surface temperature algorithm using satellite thermal data, *Journal of Geophysical Research-oceans*, *113*, C04,021, 2008.

Woollings, T., Dynamical influences on European climate: an uncertain future, *Philosophical Transactions of the Royal Society A-mathematical Physical and Engineering Sciences*, *368*, 3733–3756, 2010.

A. Münchow, College of Marine Studies, University of Delaware, Newark, Delaware, USA.

Table 1. Surface air stations and MODIS 2 km^2 box in Kennedy Channel.

Name	ID	Lon., W	Lat., N	Height, m	Time	Data
Alert	710820	62 17	82 30	66	1950-2005	6514
Alert Climate	713550	62 19	82 30	65	2006-2010	1820
Eureka	719170	85 56	79 59	10	1947-2010	19541
Grise Fjord Airport	719246	82 52	76 25	31	1978-2010	6551
Thule AFB	042020	68 30	76 32	59	1951-2010	20875
Carey Island	042030	73 00	76 38	11	1973-2010	8164
Cape Morris Jesup	043010	33 22	83 38	4	1981-2010	8370
Nord AWS	043120	16 41	81 36	34	1985-2010	7882
MODIS	n/a	66 45	80 50	0	2000-2010	1983

Table 2. MODIS Polar Cloud and Clear Sky Tests Applied.

Test	Bands	Threshold	Temperature, K	Type
1.	$6.7\mu m$	-48.5°C		Day and Night Cloud
2.	$11\mu m - 12\mu m$	2°C		Day and Night Cloud
3.	$3.9\mu m - 12\mu m$	4.5/2.0°C	235/265	Night Cloud
4a.	$11\mu m - 3.9\mu m$	-0.6/+0.8°C	235/265	Night Cloud
4b	$11\mu m - 3.9\mu m$	-11.5/-4.0°C	230/245	Day Cloud
5.	$7.2\mu m - 11\mu m$	+2/-4.5/-17.5/-21.0°C	220/245/255/265	Night Cloud
6.	$0.86\mu m$	0.08		Day Cloud
7.	$6.7\mu m - 11\mu m$	10°C		Night Clear Sky
8.	$13\mu m - 11\mu m$	3°C		Night Clear Sky
9.	$7.2\mu m - 11\mu m$	5°C		Night Clear Sky

Table 3. Statistics, Surface Air Temperature, 1987-2010 (MODIS 2000-2010). Uncertainties are at 95 % confidence assuming a decorrelation time scale of 10 days.

Name	Mean, °C	Annual, °C	Phase, Deg.	Semi-Annual, °C	Phase, Deg.	Trend, °C/year
Nuuk	-0.9 ±0.5	8.2	151	0.9	8	0.13 ±0.04
Thule AFB	-10.6 ±1.0	16.1	155	2.1	10	0.13 ±0.05
Carey Island	-8.8 ±1.0	12.3	154	1.4	20	0.07 ±0.06
Grise Fjord Airport	-13.8 ±1.4	18.9	153	1.2	44	0.13 ±0.06
Eureka	-18.4 ±1.3	22.8	159	4.1	-10	0.12 ±0.05
Alert	-16.3 ±1.3	18.7	157	3.6	-10	0.10 ±0.05
Cape Morris Jesup	-16.9 ±1.4	18.2	159	3.5	-8	0.10 ±0.06
Nord AWS	-15.6 ±1.2	17.6	159	3.9	-13	0.11 ±0.05
MODIS CASSTA	-14.7 ±2.0	12.8	152	4.3	7	0.61 ±0.24

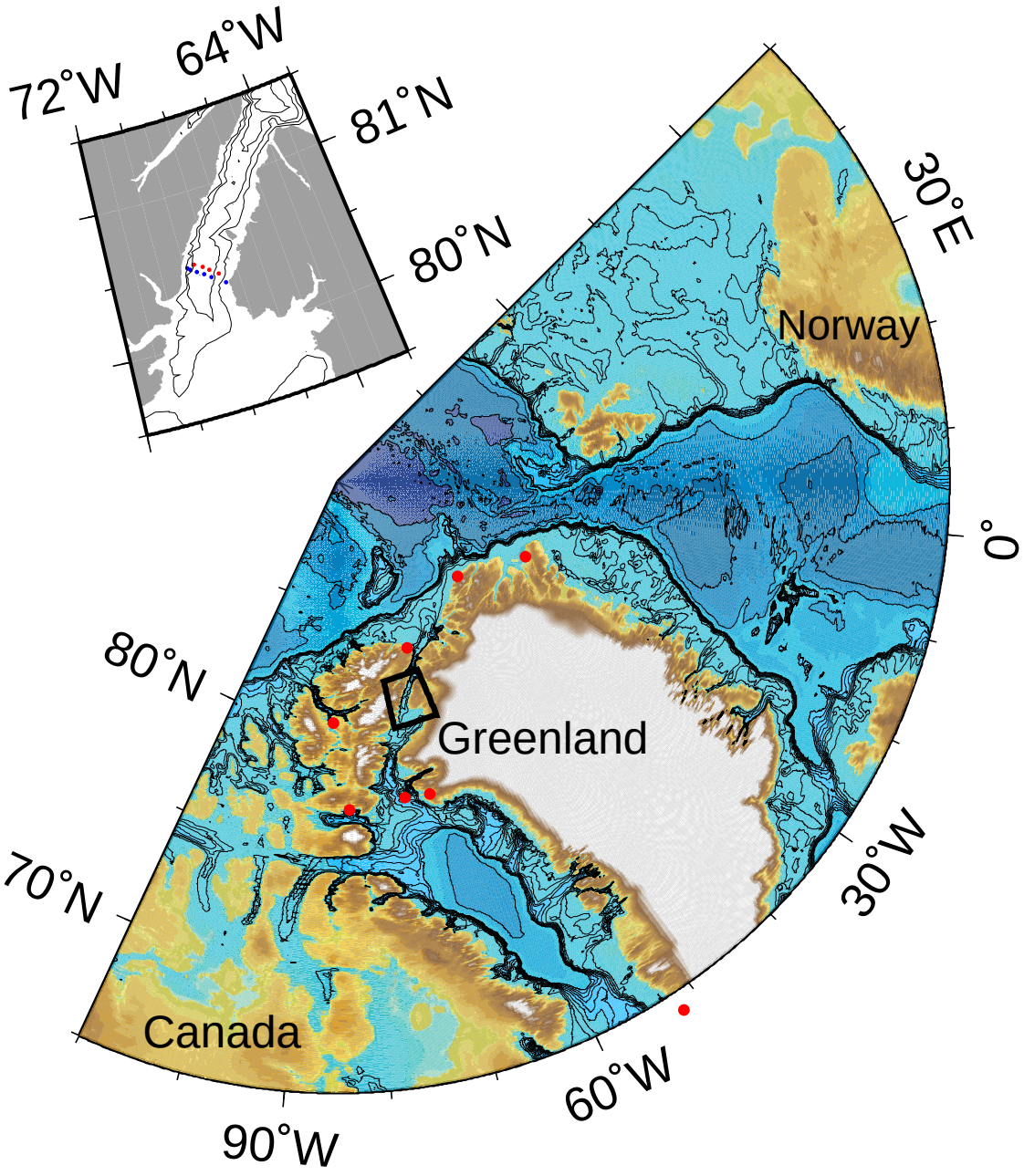

Figure 1. Map of the study area over topography. Red dots indicate meteorological surface stations while the insert shows the ocean temperature-salinity moorings for 2003-06 (blue) and 2007-09 (red). The former are offset by 0.05 degrees latitude to the south for clarity.

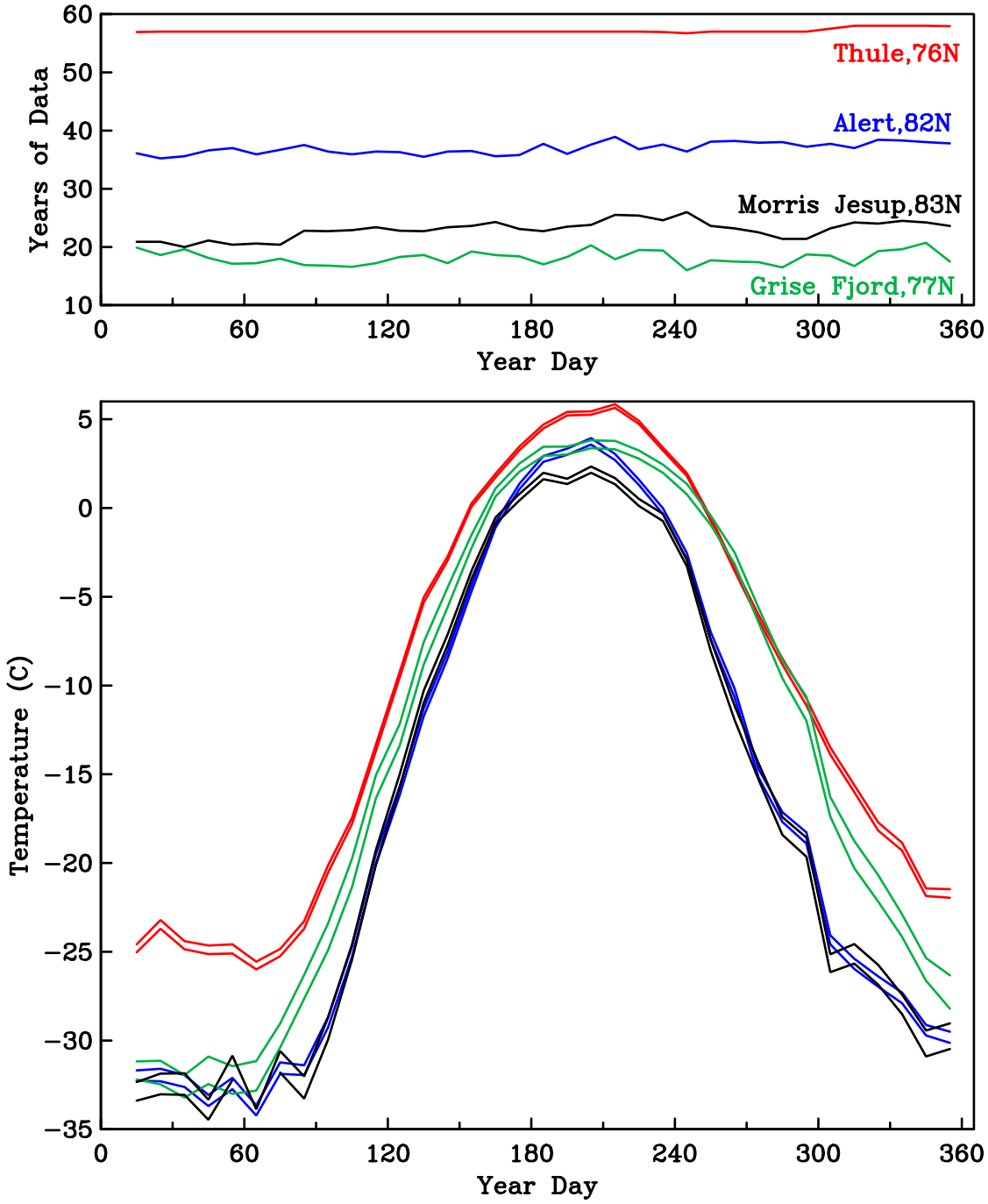

Figure 2. Annual cycle of air temperature (bottom panel) from south to north at Thule (red), Grise Fjord (green), Alert (blue), and Cap Morris Jesup. Data years (top panel) for each year day are degrees of freedom. For each location two temperature curves indicate upper and lower limits of the climatological mean temperature for that day at 95% confidence.

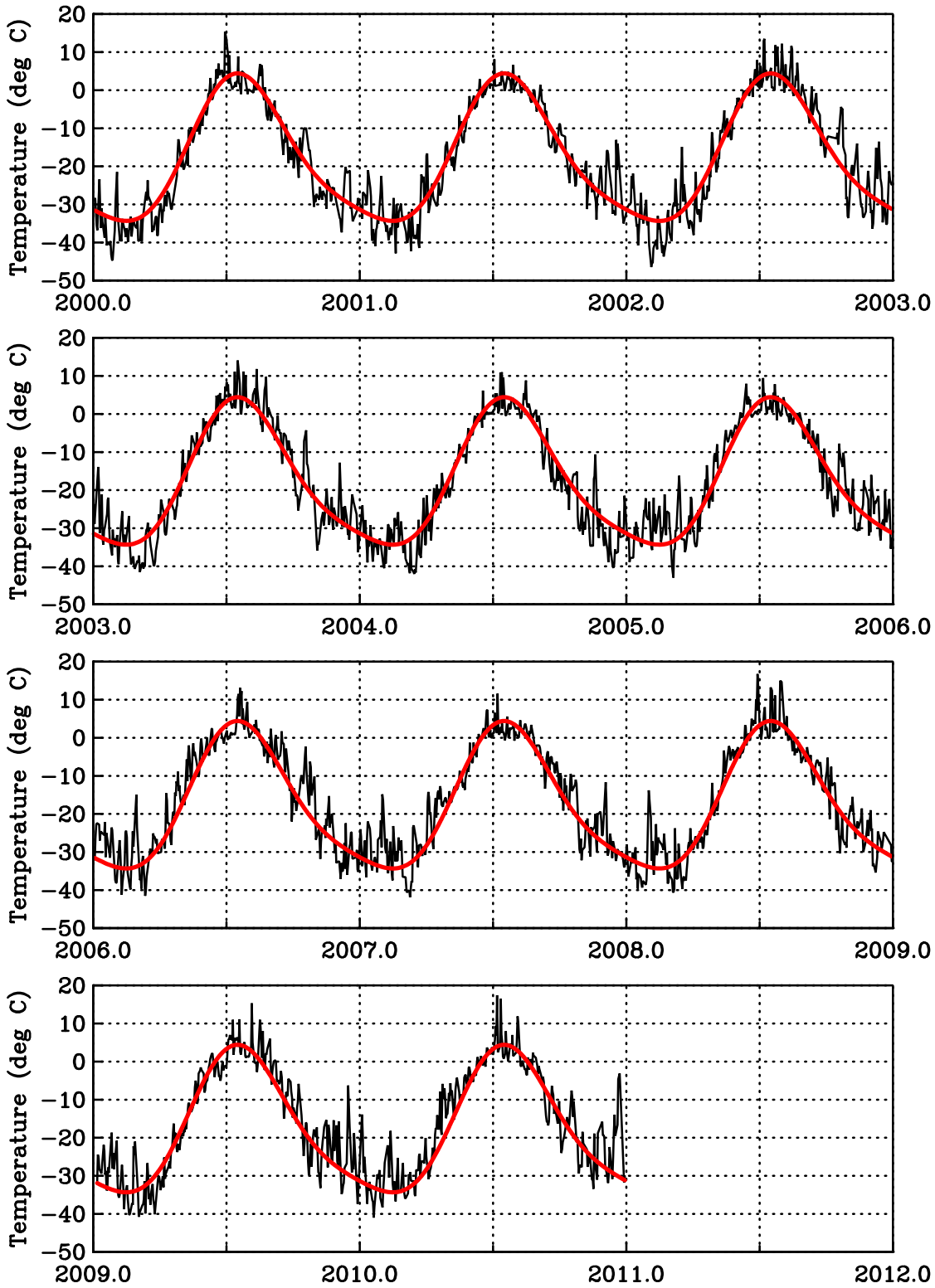

Figure 3. Surface air temperature Alert, Canada from 2000-2010 with seasonal cycle (red) determined from Eq.-1 for the 1987-2010 period.

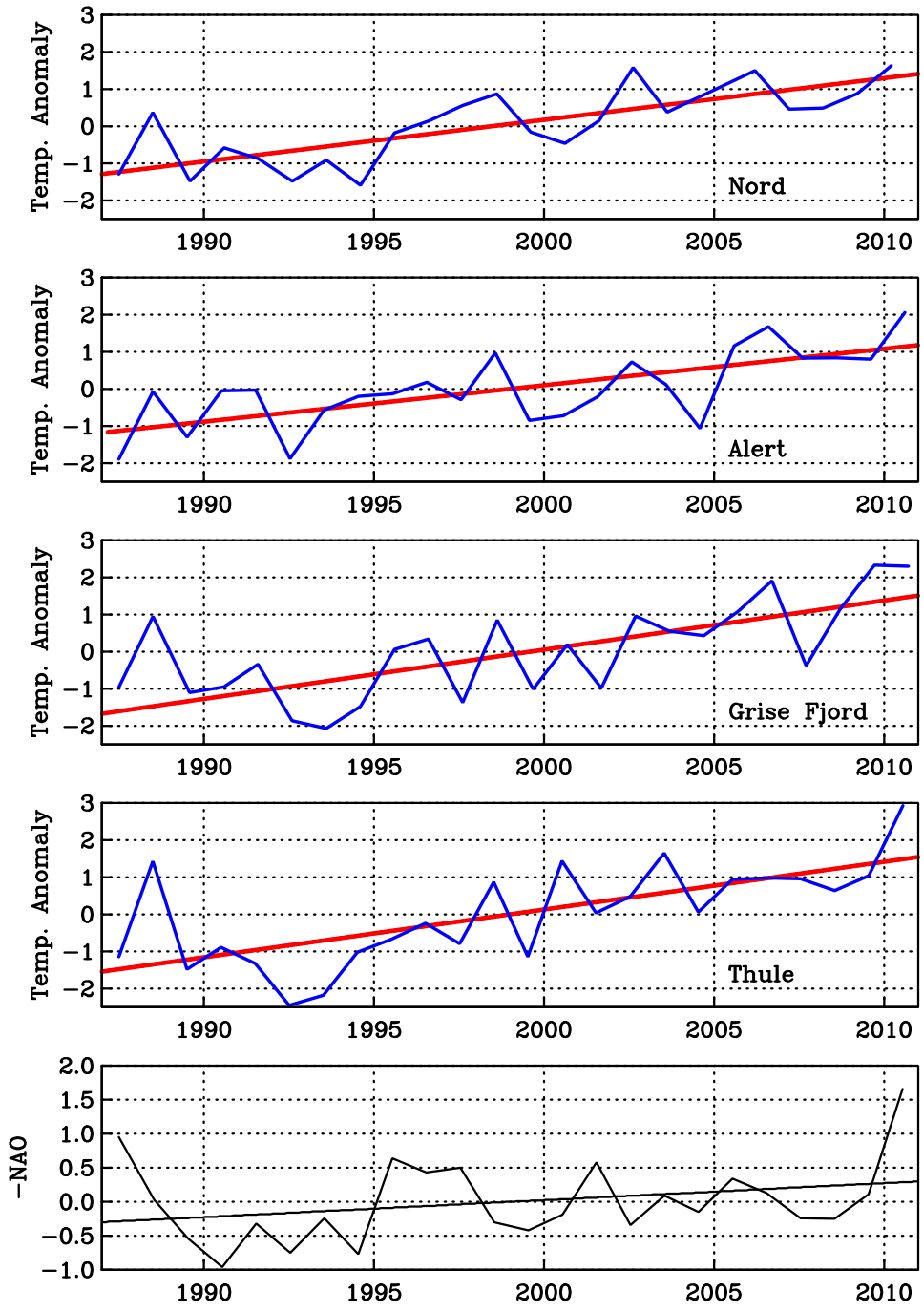

Figure 4. Annual averages and trends of air temperature anomalies for the 1987-2010 period for (top to bottom) Station Nord (Greenland), Alert (Canada), Grise Fjord (Canada), and Thule (Greenland). Bottom panel shows the North-Atlantic Oscillation Index (NAO) for the same period. All trends are significant at 95% confidence except that of NAO.

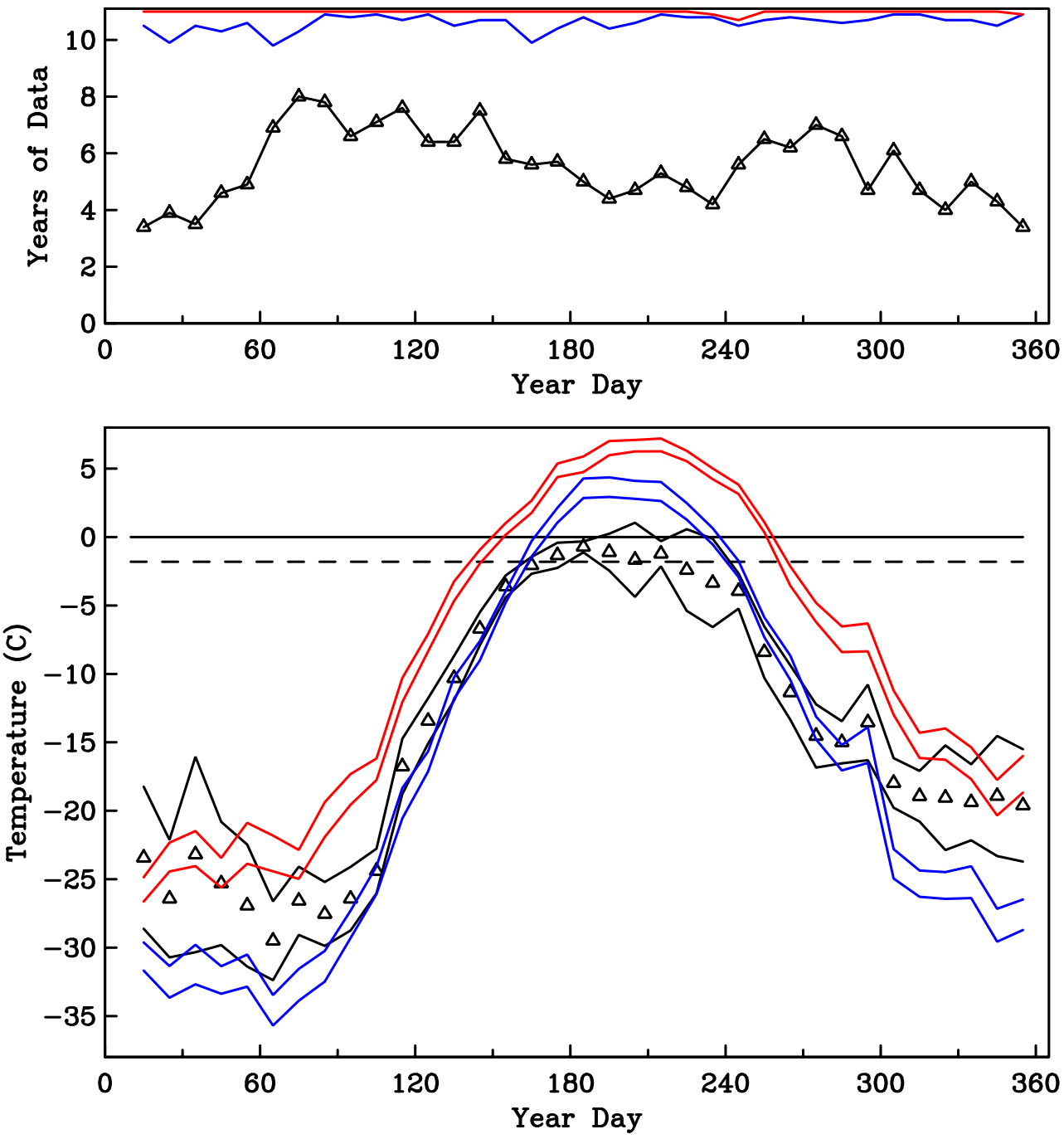

Figure 5. Annual cycle of CASSTA from a single MODIS pixel over generally ice-covered ocean in Nares Strait (black) compared with air temperature at Alert (blue) and Thule (red) for the 2000-10 period. Solid lines indicate upper and lower limits of the mean temperature for that day at 95% confidence. Each year of data is taken as a degree of freedom

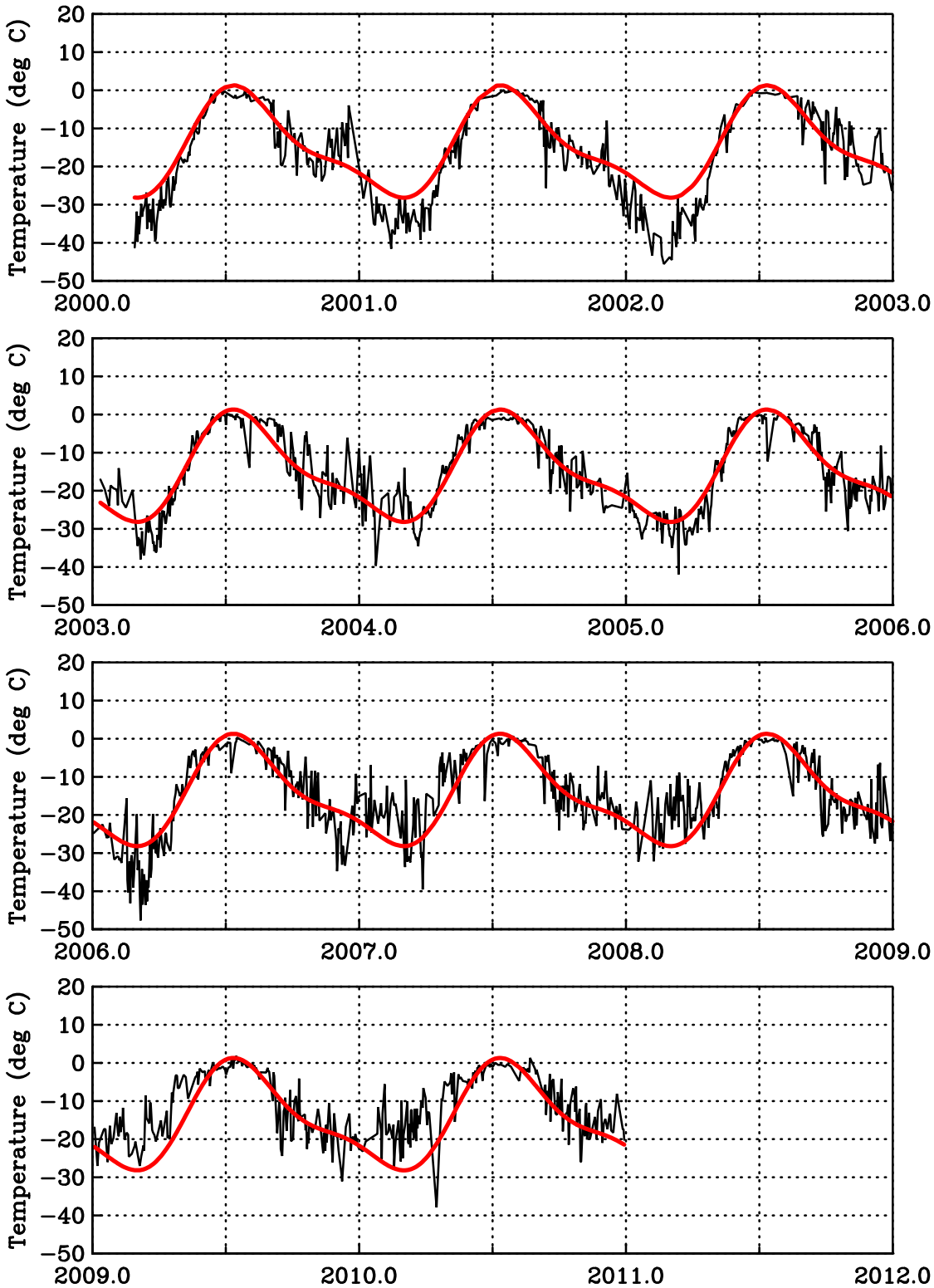

Figure 6. MODIS surface temperature from a 2 km^2 box to the west of Hans Island near the center of Nares Strait with seasonal cycle (red) determined from Eq.-1 for the 2000-2010 period.

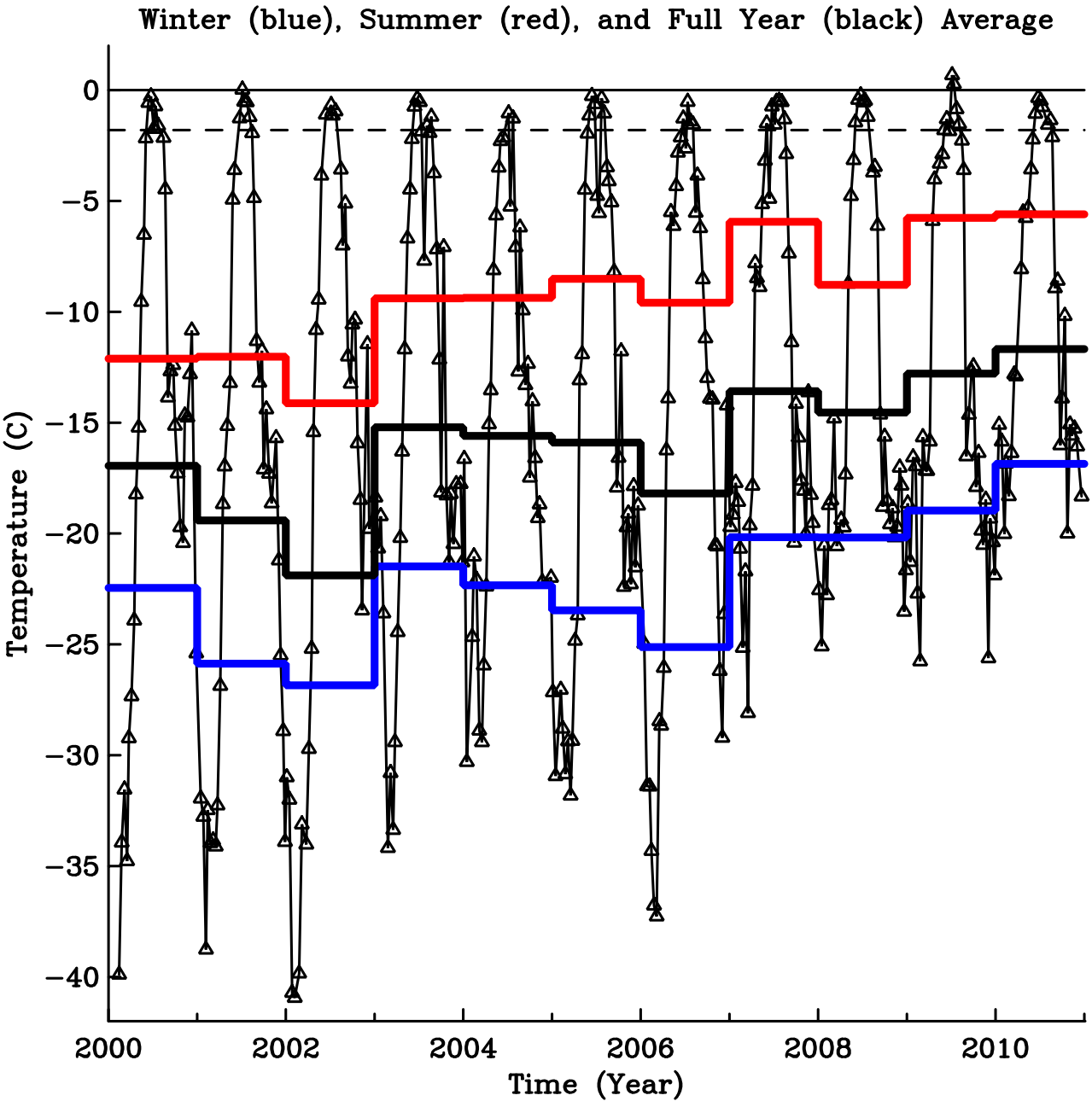

Figure 7. Time series of surface temperature from a single MODIS pixel over generally ice-covered ocean in Nares Strait. Seasonal cycles are indicated by symbols from 10-day averages while lines indicate annual averages for the calendar year (black), summer (red), and winter (blue) seasons..